Supporting Information

Hollow Core-Shell ZnO@ZIF-8 on Carbon Cloth for Flexible Supercapacitor with Ultrahigh Areal Capacitance

Xiao-Man Cao and Zheng-Bo Han*

College of Chemistry, Liaoning University, Shenyang 110036 P. R. China
* E-mail: ceshzb@lnu.edu.cn

Experimental Section

Chemicals and substrates: All the chemicals were of analytical grade and used as received without further purification. Typically, Zinc acetate dihydrate ($Zn(CH_3COO_2)\cdot 2H_2O$, 99%), 2-methylimidazole and polyvinyl alcohol (PVA) were purchased from Shanghai Macklin Biochemical Co., Ltd. Silicotungstic acid (99%) was purchased from Sinopharm Chemical Reagent Co. Ltd. *N*, *N*-dimethylformamide (DMF, 99%) and anhydrous ethanol (CH_3COOH, 99%) were purchased from Tianjin Yongda Chemical Reagent Co. Led. Aniline (Sinopharm Chemical Reagent Co., Ltd) was purified by reduced pressure distillation before use. Deionized (DI) water was used throughout all the experiments. All reagents are used without further purification. Carbon cloth was purchased from CeTech (Taiwan). The carbon cloth (1.0 cm×1.5 cm) was grafted with carboxyl and hydroxyl groups after being activated with highly concentrated nitric and sulfuric acid.

Material Synthesis

Preparation of hollow ZnO on carbon cloth:

The hollow ZnO microspheres were first rooted on carbon cloth by a hydrothermal method. Firstly, pristine carbon cloth with a mixed solution of highly concentrated nitric and sulfuric acid (V/V=3:1) was heated to reflux at 80 ^{o}C for 8 h and then adequately cleaned by deionized water before use. After that, 0.5 g of $Zn(CH_3COO_2)\cdot 2H_2O$ was stirred in an ethanol solution (15.0 mL) of 1 M silicotungstic acid for 30 min at room temperature. The activated carbon cloth was immersed in the aforementioned reaction solution. Then, the activated carbon cloth and the obtained homogeneous solution were transferred into a 25 mL Teflon-lined stainless steel autoclave and heated at 120 ^{o}C for 72 h. After the reaction, the hollow ZnO microspheres rooted on carbon cloth (ZnO-CC) was collected after washing by deionized water and ethanol for several times, and then dried at 60 ^{o}C for 12h.

Preparation of core-shell ZnO@ZIF-8 on carbon cloth:

In a typical experiment, hollow ZnO template and 0.17 g of 2-methylimidazole were added to a 25 mL Teflon-lined stainless-steel autoclave containing a mixed solvent of DMF/H_2O (16mL, 3:1 of v/v). After sonication for 15 min, the homogeneous solution was transferred to an oven preheated to 75 ^{o}C. After the mixture reacted for different reactive time, core-shell ZnO@ZIF-8 on carbon cloth (ZnO@ZIF-8-CC) was collected and washed by fresh DMF and ethanol for several times.

Preparation of polyaniline nanocoating on ZnO@ZIF-8:

Polyaniline nanocoating was prepared *via* an electrodeposition method.[1] In a typical procedure, ZnO@ZIF-8-CC was used as a working electrode. The electrolytic bath was composed of 3 M KCl solutions and 0.1 M aniline. The polymerization process of aniline was performed in a three-electrode cell at a scan rate of 30 mV s^{-1}, by the cycling of the potential between -0.2 and 1.0 V with Ag/AgCl as the reference electrode and Pt plate as the counter at 25 ^{o}C. The loading PANI was controlled by varying the electrodeposition CV segments of aniline. The resultant PANI/ZnO@ZIF-8-CC was washed by DI water for several times and dried at 80 ^{o}C.

The synthesis steps of PANI on carbon cloth (PANI-CC) and PANI/ZnO on carbon cloth (PANI/ZnO-CC) are same to PANI/ZnO@ZIF-8-CC, except without of ZIF-8 interlayer.

The mass of each component was calculated based on the mass difference before and after each step reaction. Moreover, to prevent the random error, several batches of same samples were prepared several times in parallel.

The areal mass loading of ZnO-CC is about 3.3 mg cm^{-2}. The areal mass loading of PANI(80)-CC is about 1.3 mg cm^{-2}. The areal mass loading of PANI(80)/ZnO-CC is about 4.7 mg cm^{-2}, and the mass ratio of ZnO:PANI in PANI/ZnO-CC is about 5:2. The areal mass loading of ZnO@ZIF-8-CC is about 5.3 mg cm^{-2} and the mass ratio of ZnO:ZIF-8 in ZnO@ZIF-8-CC is about 5:3. The areal mass loading of PANI(80)/ZnO@ZIF-8 is about 6.7 mg cm^{-2} and the mass ratio of ZnO:ZIF-8:PANI in PANI/ZnO@ZIF-8 is about 5:3:2.

Fabrication of the flexible supercapacitors

First, the PVA/KCl gel electrolyte was prepared by the following process. 1 g PVA powder was dissolved in 10 mL 0.02 M KCl water with vigorous stirring at 85 ^{o}C until the solution became clear. After cooling, the resulting gel was poured onto a PTFE plate and dried in air to vaporize the excess water. After solidifying at room temperature, the gel electrolyte was cut into pieces matching the size of the electrodes. The gel and the two electrodes were assembled into a sandwich structure supercapacitor. The PVA/KCl gel membrane worked as both a solid electrolyte and a separator.

Characterization:

Powder X-ray diffraction (PXRD) pattern was collected with a Bruker AXS D8 advanced automated diffractometer at 40 kV and 40 mA with Cu-Kα □radiation as the X-ray source in the 2θ range of 10-85^{o}. Scanning electron microscopy (SEM) was performed on a Hitachi SU8010 system operating at an accelerating voltage of 10.0 kV. Transmission Electron Microscopy (TEM) was performed on a Hitachi JEM-2100 system. EDS and elemental mapping patterns were acquired on the SEM (Oxford Instruments). FT-IR spectra were recorded on a Nicolet 5DX spectrometer from KBr pellets in the 4000-400 cm^{-1} range. The contact angle was measured on a Theta/Attension Optical Tensiometer (SDA 100). The specific surface area and pore structure were measured by N_2 adsorption-desorption isotherms at 77 K on a Quantachrome Autosorb-iQ Instruments. Before adsorption measurements, the samples were out-gassed under vacuum for at least two hours at 200 ^{o}C. The specific surface area of the samples was calculated using the Brunauere-Emmette-Teller (BET) method. The cumulative pore volume and pore size distributions evaluated by Non-Local Density Functional Theory (NLDFT, nitrogen on carbon, slit/cylinder pores.QSDFT equilibrium model). The total pore volume was estimated from the amount adsorbed at a relative pressure of about 0.995. The primary mesopore volume (V_p), and micropore volume (V_{mi}), were respectively evaluated using the α_s-plot method with the relationship of as with relative pressure p/p_0 defined by the equation: α_s = 0.1385(60.65/(0.03071-ln(p/p0)))^0.3968.[2] The V_{mi} was calculated using the standard reduced adsorption, α_s, interval from about 0.8 to 1.2 and from about 1.8 to 2.2 for the calculation of V_{mi+me}. XPS was collected on the PHI Quantum 2000 spectrometer (Quantum 2000, USA) using monochromated X-rays from an Al K source with a takeoff angle of 45° from the surface plane.

Electrochemical Performance Measurements

The electrochemical performance of the as-prepared electrodes were studied in a three-electrode cell using Ag/AgCl as the reference electrode and Pt plate as the counter electrode with 3 M KCl electrolyte solution. All electrochemical measurements were carried out at room temperature by using a CHI660E electrochemical workstation (Shanghai Chenhua Instruments Co., China). Symmetric flexible supercapacitor devices were assembled with PANI/ZnO@ZIF-8-CC electrodes. PVA/KCl gel was sandwiched between the electrodes as the separator and electrolyte. The electrochemical properties of the devices were measured by a two-electrode system using a CHI660E electrochemical workstation (Shanghai Chenhua Instruments Co., China). Electrochemical impedance spectroscopy (EIS) was performed at open circuit voltage (-0.02 V) within the frequency range of 10^{-2} to 10^{4} Hz and 0.005 V amplitude (alternate current amplitude).

Calculation formulas

The areal capacitance calculated from CV tests can be calculated from the following formula (1):

$$C = \frac{1}{vs(V_b - V_a)}\int_{V_a}^{V_b} IdV \qquad (1)$$

where C (F cm^{-2}) is the areal capacitance, s (cm^{-2}) is the apparent area of active materials loaded in working electrode, v (V s^{-1}) represents the scan rate, V_b and V_a are high and low voltage limit and I (A) is the instant current on CV curves.

As for gravimetric capacitance, formula (1) can be changed to be the following formula (2):

$$C = \frac{1}{vm(V_b - V_a)} \int_{V_a}^{V_b} I dV \qquad (2)$$

where m is the mass of activated material on a working electrode.

The areal capacitance derived from GCD tests was calculated on the basis of the discharge profile according to formula (3):

$$C = \frac{I \times \Delta t}{s \times \Delta V} \qquad (3)$$

where C (F cm^{-2}) is the areal capacitance, I (A) refers to the discharge current, Δt (s) represents the discharge time and ΔV (V) is the range of charge-discharge voltage.

The energy density (E) was determined by formula (3) and (4):

$$E = \frac{1}{2} \times C \times \Delta V^2 \qquad (4)$$

The power density (P) was determined by formula (4):

$$P = \frac{E}{\Delta t} \qquad (5)$$

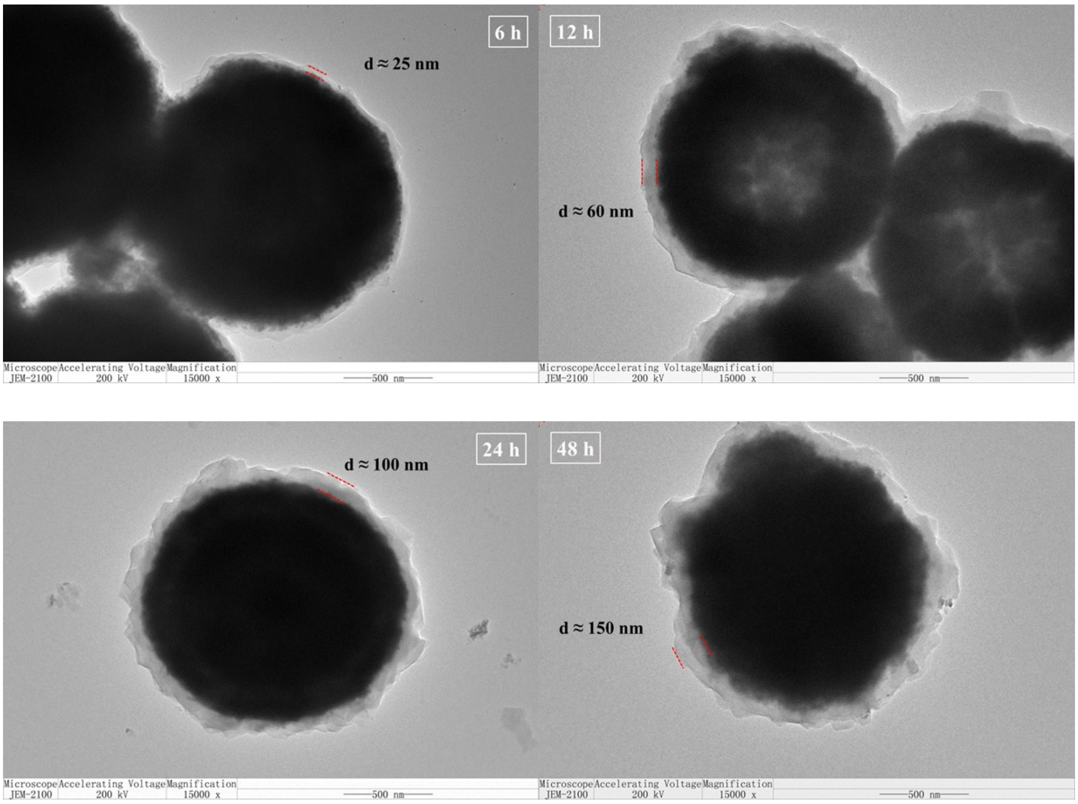

Fig. S1 TEM images of ZnO cores with ZIF-8 shells following various reaction times.

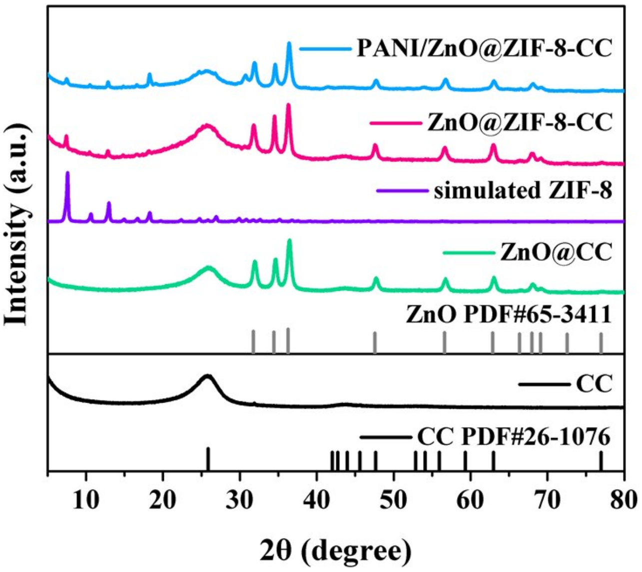

Fig. S2 XRD patterns of the activated CC, ZnO-CC, ZnO@ZIF-8-CC and PANI/ZnO@ZIF-8-CC composites.

The FT-IR spectrum of PANI/ZnO@ZIF-8 exhibits typical PANI peaks, indicating ZnO@ZIF-8 and PANI are assembled together. Several characteristic peaks associated with the amide group can be observed. The main peaks of PANI located at 1557 and 1494 cm^{-1} can be assigned to the C=C stretching vibrations of quinine and benzene brings, respectively. The band at 1299 cm^{-1} corresponds to the C-N or C-N^{+} stretching vibration. The peak at 811 cm^{-1} is attributed to the out-of-plane bending of C-H.[3] For ZnO@ZIF-8, the peaks at 419 and 1583 cm^{-1} correspond to the stretching vibrations of Zn-N and C-N. The peaks at 753, 1145, 1307 and 1459 cm^{-1} correspond to the characteristic absorption peaks of the imidazole ring.[4] For PANI/ZnO@ZIF-8, the main characteristic peaks of PANI still appear and shift to a relatively higher wavenumbers. All of the above peaks show that PANI exists in PANI/ZnO@ZIF-8 and demonstrate the presence of the interactions between ZnO@ZIF-8 and PANI.

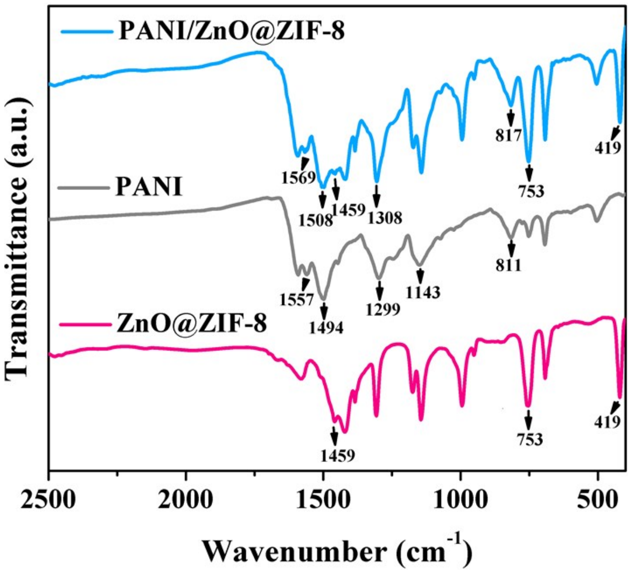

Fig. S3 FT-IR spectrum of ZnO@ZIF-8, pure PANI and PANI/ZnO@ZIF-8.

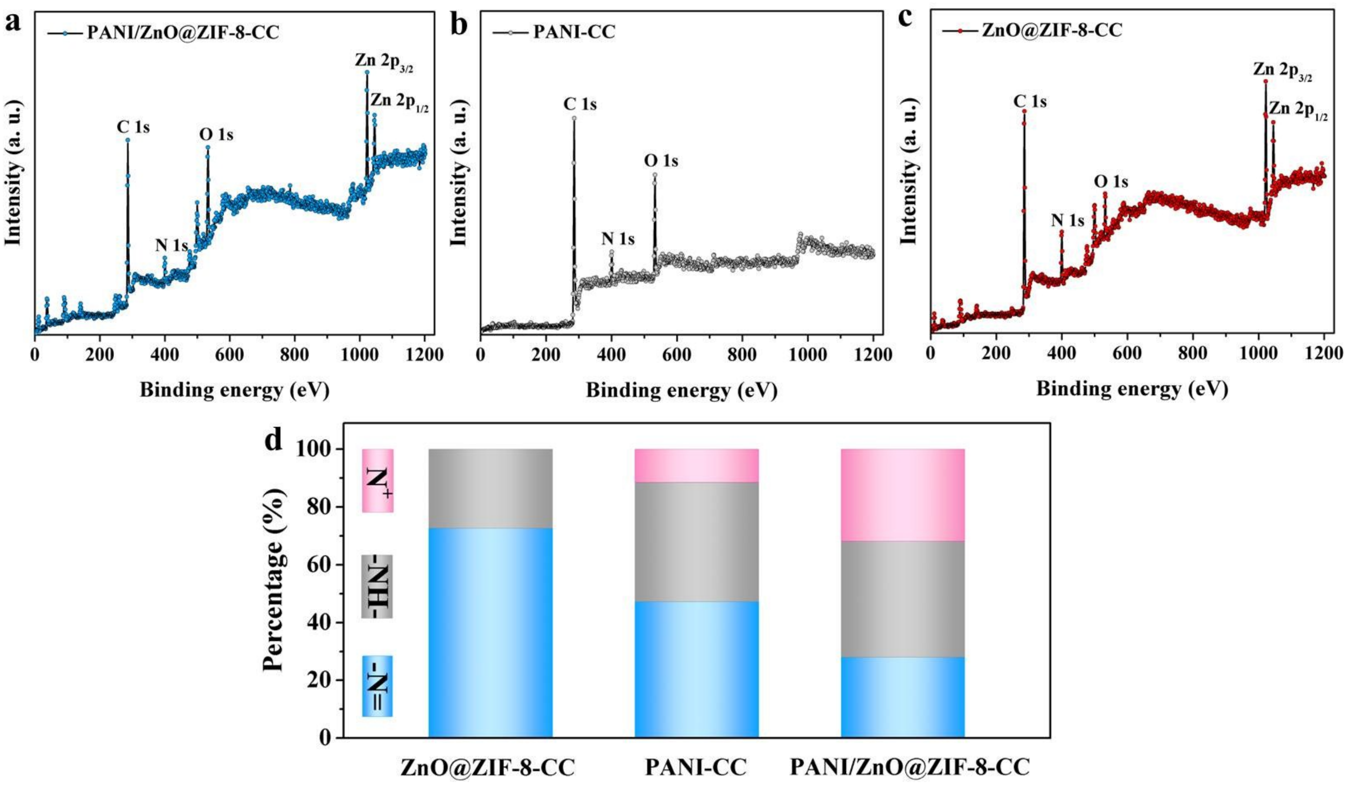

Fig. S4 XPS full-scan spectra and N 1s spectra of (a) PANI/ZnO@ZIF-8-CC, (b) PANI-CC and (c) ZnO@ZIF-8-CC; (d) Distribution of quinoid amine (=N-), benzenoid amine(-NH-) and positively charged imine and protonated amine (N$^+$).

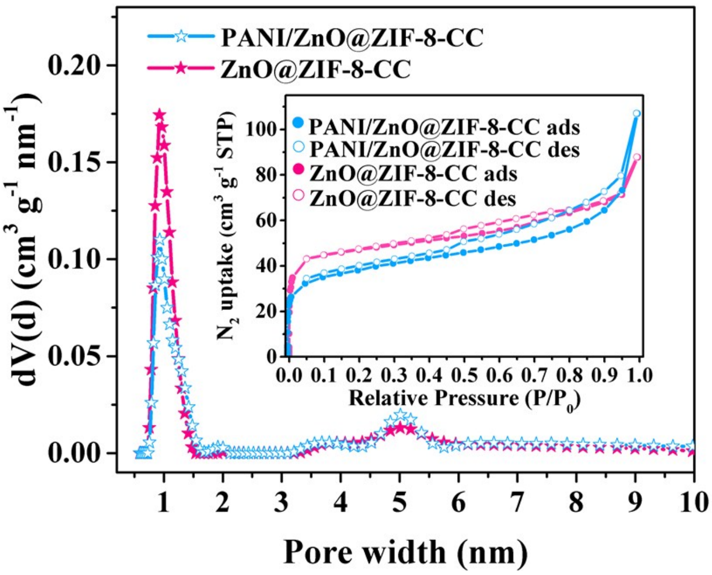

Fig. S5 N^2 adsorption-desorption isotherms and pore size distribution for the samples.

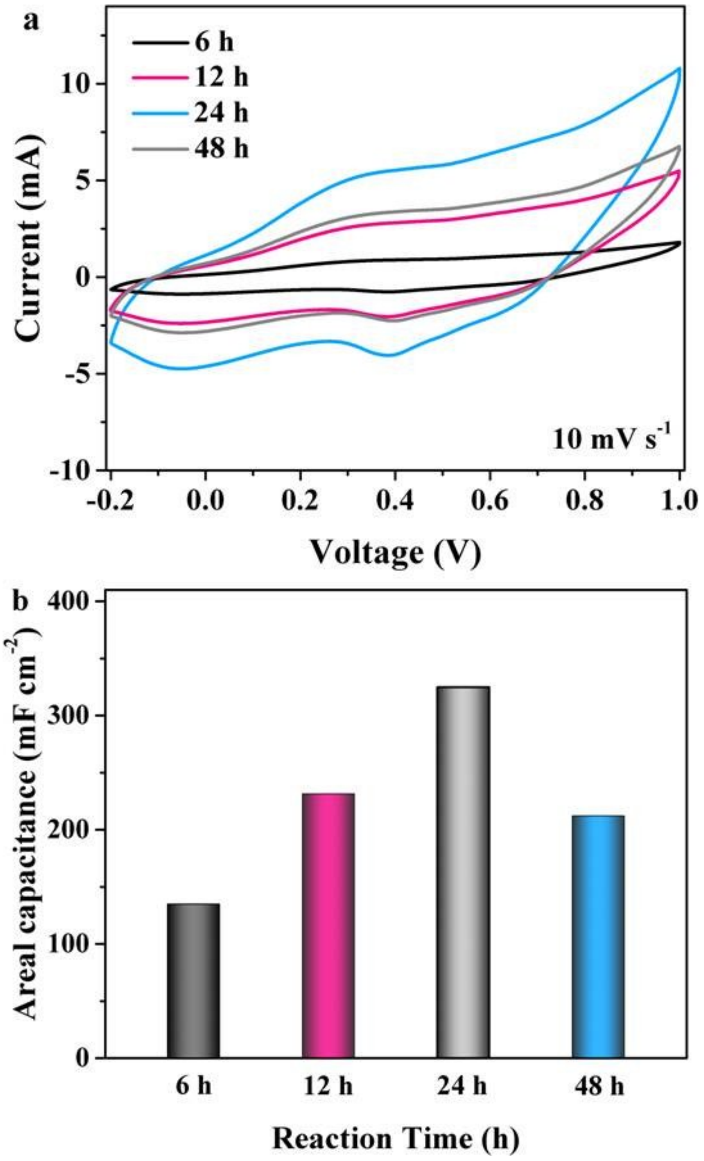

Fig. S6 CV curves (a) and the areal capacitances (b) for ZnO@ZIF-8 samples with various reaction times.

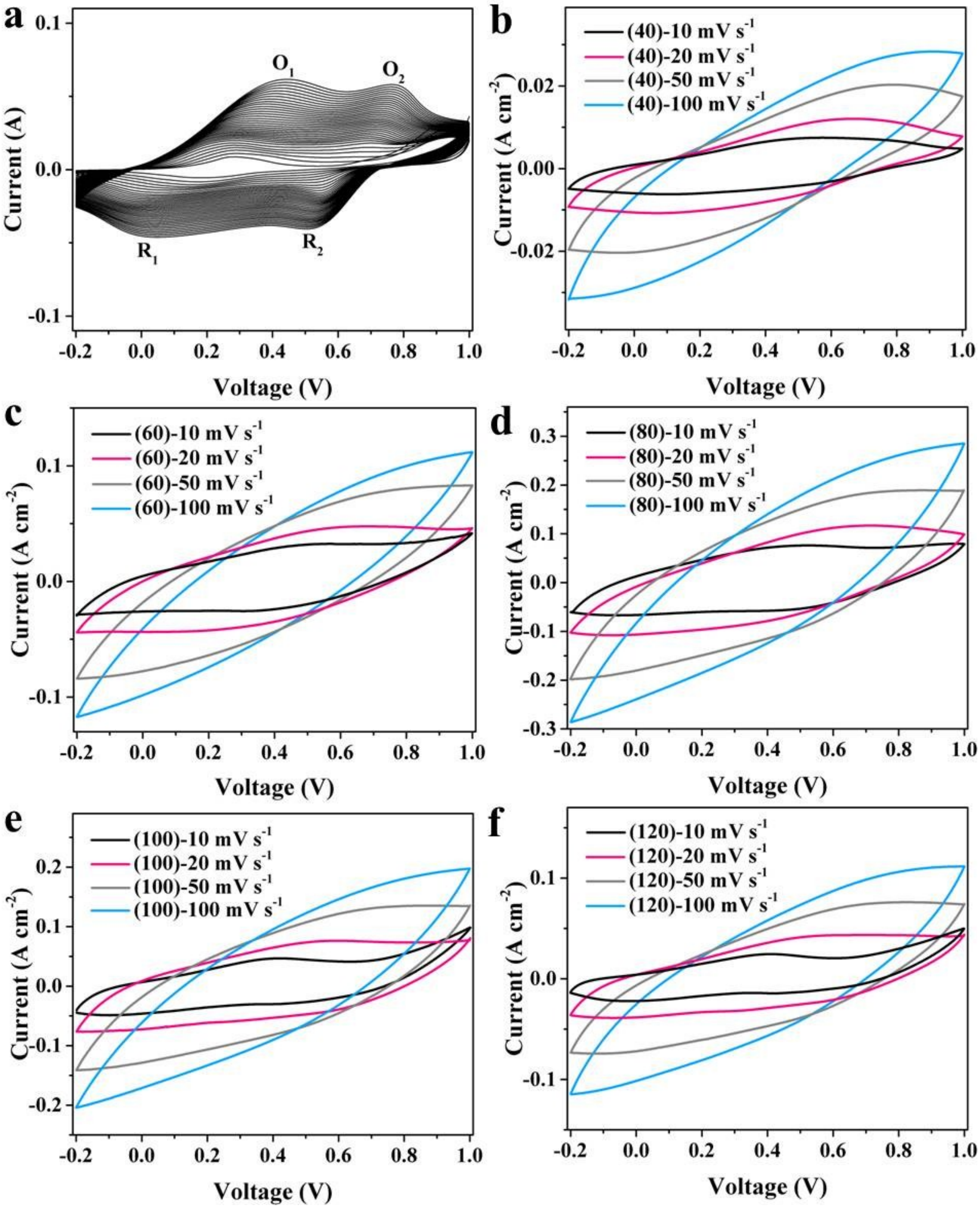

Fig. S7 (a) CV curves of electropolymerization process of aniline onto ZnO@ZIF-8-CC; (b-f) CV curves for PANI/ZnO@ZIF-8 samples with different deposition cycle numbers of PANI;

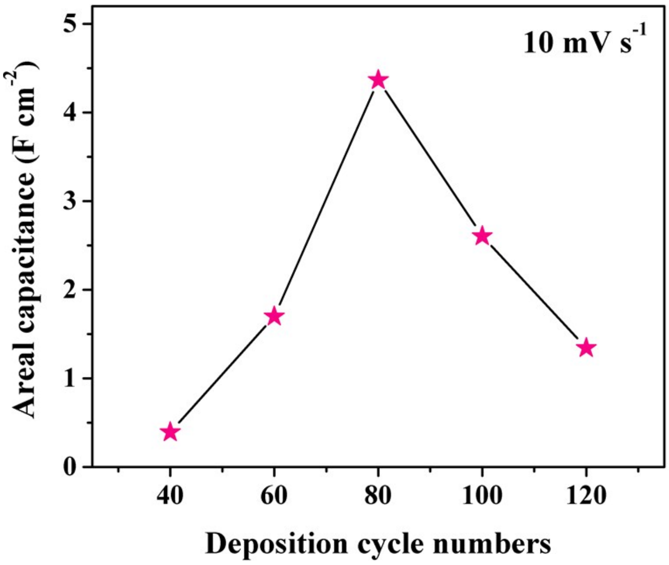

Fig. S8 Area capacitance with respect to different deposition cycle numbers of PANI at a scan rate of 10 mV s^{-1}.

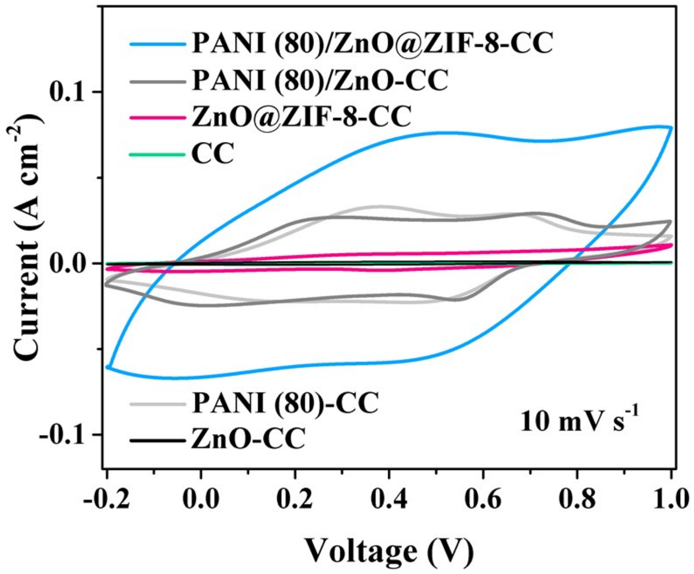

Fig. S9 CV profiles of PANI(80)/ZnO@ZIF-8-CC, PANI(80)/ZnO-CC, PANI(80)-CC, ZnO@ZIF-8-CC, ZnO-CC and actived CC electrodes at 10 mV s^{-1}.

Table S1. Comparison of our flexible supercapacitors with other reports in terms of electrode areal capacitance.

Electrode Materials	Current density (A cm^{-2})/ Scan rate (mV s^{-1})	Electrolyte	Capacitance [mF cm^{-2}]	Configuration	Ref.
PANI/CNTs/G/PETC	1.5 mA cm^{-2}	1 M H_2SO_4	791	three-electrode	5
PEDOT/H-15G-CNTF	10 mV s^{-1}	3 M KCl	128	three-electrode	6
Co-Mn MOF	1 mA cm^{-2}	1 M KOH	1318	three-electrode	7
PEDOT-GO/U-C	10 mV s^{-1}	3 M KCl	102	three-electrode	8
PANI-ZIF-67-CC	10 mV s^{-1}	3 M KCl	2140	three-electrode	9
PANI(80)/ZnO-CC	10 mV s^{-1}	3 M KCl	1491	three-electrode	*
PANI(80)-CC	10 mV s^{-1}	3 M KCl	1470	three-electrode	*
ZnO@ZIF-8-CC	10 mV s^{-1}	3 M KCl	325.6	three-electrode	*
PANI/ZnO@ZIF-8-CC	10 mV s^{-1}	3 M KCl	4370	three-electrode	This work
PANI/ZnO@ZIF-8-CC	5 mA cm^{-2}	3 M KCl	4839	three-electrode	This work

*Control experiment

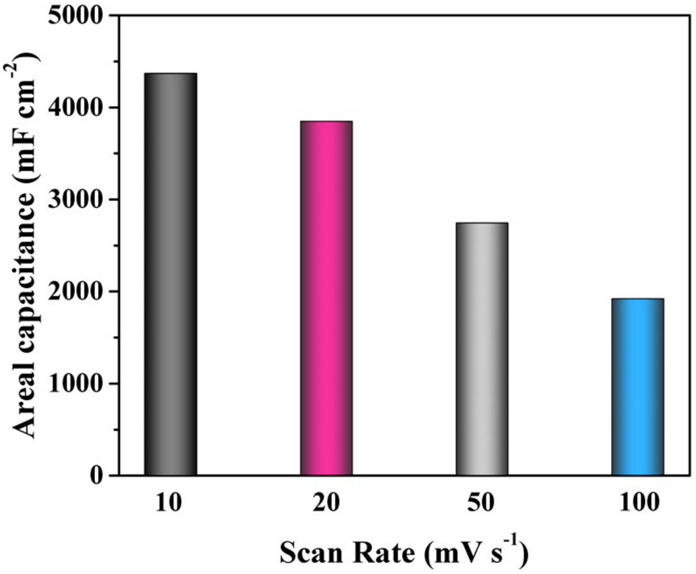

Fig. S10 Areal capacitance of PANI/ZnO@ZIF-8-CC at different scan rates from 10 to 100 mV s^{-1}.

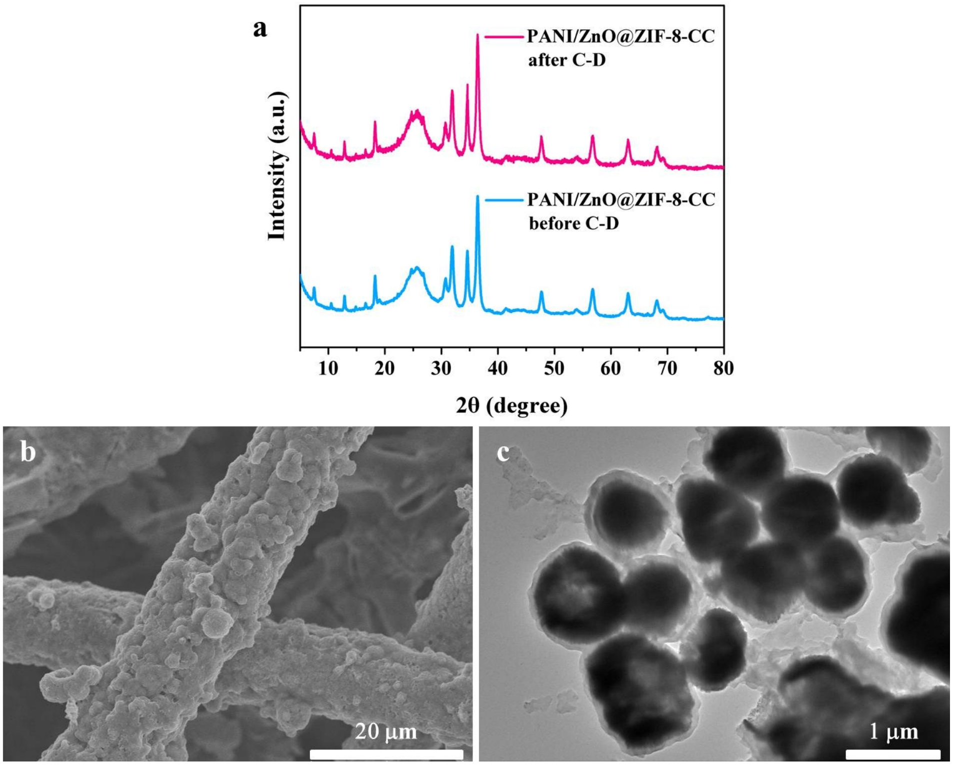

Fig. S11 The XRD patterns (a); SEM (b) and TEM (c) images of the PANI(80)/ZnO@ZIF-8-CC electrode after the long-term charge-discharge process.

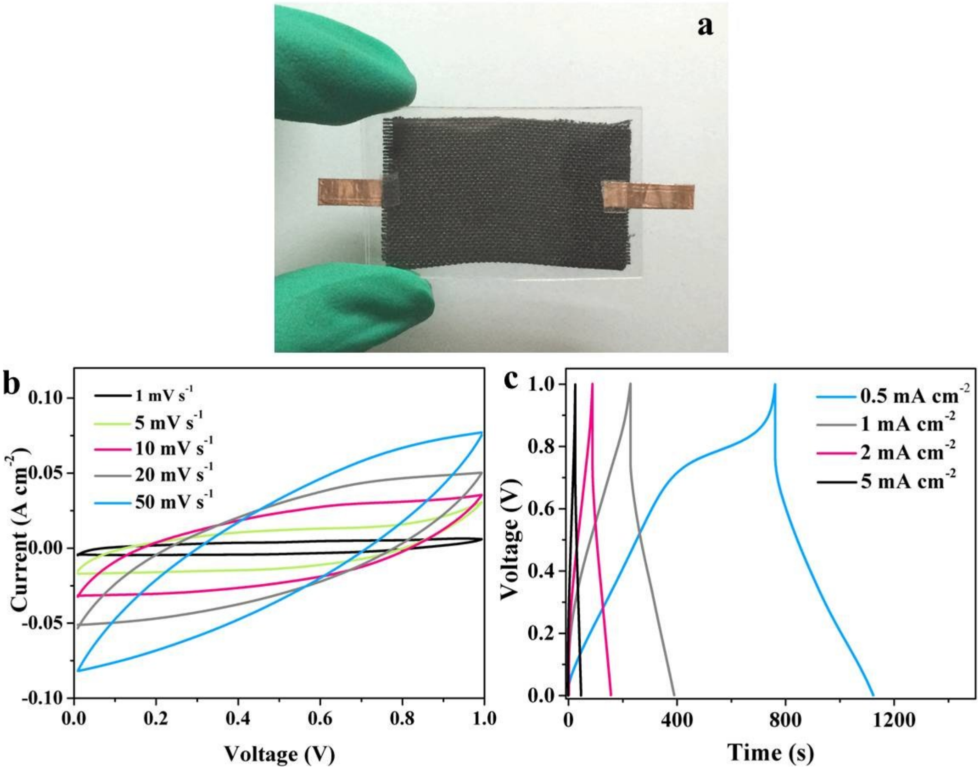

Fig. S12 (a) Optical image of the flexible supercapacitors device; (c) CV curves; (d) GCD curves of the device.

Supporting references

(1) C. Lu, T. Ben, S. Xu, S. Qiu, *Angew. Chem. Int. Ed.,* 2014, ***53***, 6545-6458.
(2) M. Kruk, M. Jaroniec, *Chem. Mater.,* 2000, ***12***, 1961-1968.
(3) R. R. Salunkhe, J. Tang, N. Kobayashi, J. Kim, Y. Ide, S. Tominaka, J. H. Kim, Y. Yamauchi, *Chem. Sci.,* 2016, *7*, 5704-5713.
(4) X. B. Yang, Z. D. Wen, Z. L. Wu, X. T. Luo, *Inorg. Chem. Front.,* 2018, ***5***, 687-693.
(5) 24d) L. N. Jin, F. Shao, C. Jin, J. N. Zhang, P. Liu, M. X. Guo, S. W. Bian, *Electrochim Acta,* 2017, ***249***, 387-394.
(6) 24c) D. Y. Fu, H. W. Li, X. M. Zhang, G. Han, H. H. Zhou, Y. Z. Chang, *Mater. Chem. Phys.,* 2016, ***179***, 166-173.
(7) b) S. H. Kazemi, B. Hosseinzadeh, H. Kazemi, M. A. Kiani, S. Hajati, *ACS Appl. Mater. Interfaces,* 2018, ***10***, 23063-23073.
(8) 24a) D. Y. Fu, H. H. Zhou, X. M. Zhang, G. Y. Han, Y. Z. Chang, H. W. Li, *Chemistry Select,* 2016, ***2***, 285-289.
(9) L. Wang, X. Feng, L. T. Ren, Q. H. Piao, J. Q. Zhong, Y. B. Wang, H. W. Li, Y. F. Chen, B. Wang, *J. Am. Chem. Soc.,* 2015, ***137***, 4920-4923.